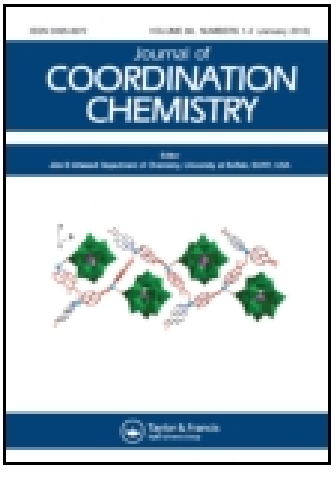

Journal of Coordination Chemistry
Publication details, including instructions for authors and subscription information:
http://www.tandfonline.com/loi/gcoo20

Synthesis, crystal structure, and SOD-like activity of two copper(II) complexes with hydroxymethyl pendants

Ying-Hua Zhou[ab], Da-Liang Sun[a], Jun Tao[a], Li-Qing Chen[a], Ya-Fan Huang[a], Ying-Kun Li[a] & Yong Cheng[ac]

[a] College of Chemistry and Materials Science, Anhui Normal University, Wuhu, PR China

[b] Center for Nano Science and Technology, Anhui Normal University, Wuhu, PR China

[c] The Key Laboratory of Functional Molecular Solids, Ministry of Education, Anhui Normal University, Wuhu, PR China

Accepted author version posted online: 30 Jun 2014.Published online: 22 Jul 2014.

To cite this article: Ying-Hua Zhou, Da-Liang Sun, Jun Tao, Li-Qing Chen, Ya-Fan Huang, Ying-Kun Li & Yong Cheng (2014) Synthesis, crystal structure, and SOD-like activity of two copper(II) complexes with hydroxymethyl pendants, Journal of Coordination Chemistry, 67:14, 2393-2404, DOI: 10.1080/00958972.2014.940335

To link to this article: http://dx.doi.org/10.1080/00958972.2014.940335

Journal of Coordination Chemistry, 2014
Vol. 67, No. 14, 2393–2404, http://dx.doi.org/10.1080/00958972.2014.940335

Synthesis, crystal structure, and SOD-like activity of two copper(II) complexes with hydroxymethyl pendants

YING-HUA ZHOU*†‡, DA-LIANG SUN†, JUN TAO†, LI-QING CHEN†, YA-FAN HUANG†, YING-KUN LI† and YONG CHENG†§

†College of Chemistry and Materials Science, Anhui Normal University, Wuhu, PR China
‡Center for Nano Science and Technology, Anhui Normal University, Wuhu, PR China
§The Key Laboratory of Functional Molecular Solids, Ministry of Education, Anhui Normal University, Wuhu, PR China

(*Received 8 March 2014; accepted 6 June 2014*)

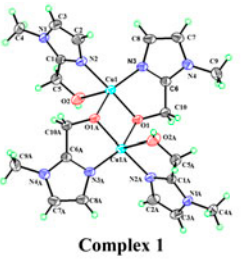

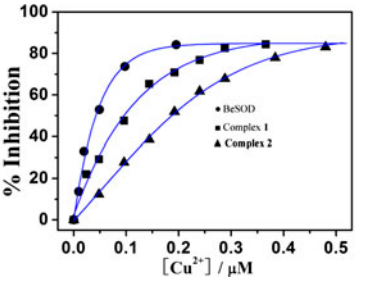

Dinuclear and mononuclear copper(II) complexes (**1**, $[Cu_2(HL)_2(L)_2](ClO_4)_2$; **2**, $[Cu(HL)_2(phen)](ClO_4)_2$, where HL = (*N*-methyl-2-methylol)imidazole, phen = 1,10-phenanthroline) have been synthesized and characterized by single crystal X-ray diffraction. The SOD-like activity (IC_{50}) of **1** and **2** were measured to be 0.10 ± 0.01 and 0.19 ± 0.01 μM by NBT assay at pH 7.8. The higher SOD activity of **1** could be contributed to the coordination configuration and the labile hydroxymethyl pendants. Electrochemistry and the frontier molecular orbital energies of the complexes were also studied.

To mimic the active site of Cu,Zn-SOD, new copper(II) complexes (**1**, $[Cu_2(HL)_2(L)_2](ClO_4)_2$; **2**, $[Cu(HL)_2(phen)](ClO_4)_2$; where HL = (*N*-methyl-2-methylol)imidazole, phen = 1,10-phenanthroline) have been synthesized and characterized by elemental analysis, IR, and single-crystal X-ray diffraction. Copper(II) in **1** is four-coordinate by a N_2O_2 plane with two copper(II) ions bridged with two oxygens from the deprotonated hydroxylmethyl pendants. Each Cu^{2+} in **2** is coordinated by four nitrogens from two HL and one co-ligand of 1,10-phenanthroline. Electrochemistry of the complexes was studied by cyclic voltammetry. The atomic net charges distribution and frontier molecular orbital energies were obtained by Gaussian 98 program with DFT method at B3LYP/lanl2dz level. The SOD-like activity (IC_{50}) of **1** and **2** were measured as 0.10 ± 0.01 and 0.19 ± 0.01 μM by NBT assay at pH 7.8. The higher SOD activity of **1** could be attributed to the coordination configuration and the labile hydroxymethyl pendants.

Keywords: Copper complex; Crystal structure; Superoxide dismutase; Imidazole; Mimic

*Corresponding author. Email: yhzhou@mail.ahnu.edu.cn

1. Introduction

Superoxide anion ($O_2^{\cdot-}$) is a natural byproduct of the normal metabolism of oxygen and has the important functions of cell signaling and homeostasis. However, during environmental stress, the level of $O_2^{\cdot-}$ can increase dramatically, inducing host molecular and cellular damages to lipids and proteins [1–3]. Copper, zinc superoxide dismutase (Cu,Zn-SOD) is an ubiquitous enzyme with an essential role in antioxidant defense through catalyzing the dismutation of $O_2^{\cdot-}$ to hydrogen peroxide and dioxygen under physiological conditions [4, 5]. Due to limitations such as solution instability, immunogenicity, bell-shaped dose response curves, short half-lives, costs of production and proteolytic digestion, the direct utilization of such enzyme as pharmaceutical agents still has many problems [6]. Therefore, research of Cu,Zn-SOD mimic has been carried out towards obtaining stable, nontoxic, and inexpensive low molecular weight biomimetic molecules, which are able to catalyze superoxide dismutation and provide important therapeutic applications [7]. To mimic Cu,Zn-SOD, many copper(II) complexes with polyamine and porphyrin derivative ligands were reported. However, the SOD-like activities of mimics were relatively low and the water solubility of mimics should be improved [8–11]. Imidazole compounds widely exist in metalloenzymes of mammals due to coordination diversity and favorable hydrophilicity [12–14]. The flexible hydroxymethyl arm can be expected to adapt to the different requirements of configuration and proper basicity for copper ions. Furthermore, oxygen of the hydroxymethyl arm may mimic the role of water molecule bound to the copper site of Cu_2,Zn_2-SOD [15]. Metal hydroxides and alkoxides play important roles on activation of metal proximate alcoholic OH groups in carbonic anhydrase and carboxypeptidase [16, 17]. Therefore, we herein synthesize two di/mono-copper(II) complexes based on the imidazole derivative containing hydroxymethyl pendant groups (**1**, $[Cu_2(HL)_2(L)_2](ClO_4)_2$; **2**, $[Cu(HL)_2(phen)](ClO_4)_2$; where HL = (*N*-methyl-2-methylol)imidazole, phen = 1,10-phenanthroline), which have been characterized by X-ray crystallography. The atomic net charge distribution and frontier molecular orbital energies were obtained by Gaussian 98 with the DFT method at B3LYP/lanl2dz level. Moreover, the electrochemistry and SOD activity of **1** and **2** were determined.

2. Experimental

Caution: Although no problems were encountered in this work, transition-metal perchlorate salts are potentially explosive and should thus be prepared in small quantities and handled with care.

2.1. *Materials and instrumentation*

Organic reagents were reagent grade and solvents used in this research were purified by standard procedures. Water used in all physical measurement experiments was double distilled. An improved method of solvothermal synthesis has been applied for the preparation of (*N*-methyl-2-methylol)imidazole from *N*-methyl-1H-imidazole with a higher yield, and was confirmed by elemental analyses and ^{1}H NMR spectra [18, 19]. Then, the mono- or dinuclear complexes were synthesized by reaction of ligand and copper(II) perchlorate. Elemental analyses for C, H, and N were obtained on a Vario EL III. Infrared spectroscopy on

KBr pellets was performed on a Shimadzu IR Prestige-21 infrared spectrophotometer from 4000–400 cm^{-1}. Electronic spectra were measured on a Shimadzu UV-2450 spectrophotometer. The redox potentials of the complexes were determined by CH Instrument 400c using the conventional three-electrode system of glass carbon electrode as the working electrode, platinum wire as the counter electrode, and Ag/AgCl electrode as the reference electrode. All electrospray ionization mass spectrometry measurements were carried out using a Finnigan LCQ DECA XP PLUS ion trap spectrometer operating in the positive ion mode and equipped with an orthogonal ESI source (Thermo Electron Corporation, USA).

2.2. *Synthesis of (N-methyl-1H-imidazol-2-yl)methanol (HL)*

To a solution of *N*-methyl-1H-imidazole (15.00 g, 0.18 M) in 20 mL anhydrous acetonitrile in a 100 mL polytetrafluoroethylene flask was added a solution of paraformaldehyde (30.00 g, 1.00 M) in 20 mL anhydrous acetonitrile with vigorous stirring under nitrogen. After placing in the sealed high pressure reactor and heating to 393 K for 16 h, the reaction was cooled to room temperature and evaporated under reduced pressure to dryness. The residue was poured into acetone (100 mL) to give a precipitate. The crude product was recrystallized from a solution of ethyl acetate and anhydrous methanol (*v*/*v*, 2 : 1). Colorless cubic crystals suitable for X-ray analysis were obtained in 92% yield. Anal. Calcd for $C_5H_8N_2O$: C, 53.56; N, 24.98; H, 7.19%. Found: C, 53.36; N, 24.88; H, 7.31%. ^{1}H NMR (300 MHz, $CDCl_3$): δ_H 6.86 (2H; CH-4,5), 4.63 (2H; CH_2), 3.73 (3H, CH_3); ^{13}C NMR (500 MHz, D_2O): δ_C 32.74 (–CH_3), 55.08 (CH_2OH), 123.28 (CH-5), 126.32 (CH-4), 146.92 (CH-2).

2.3. *Synthesis of $[Cu_2(HL)_2(L)_2](ClO_4)_2$ (1)*

To 10 mL methanol solution of HL (0.224 g, 2.0 mM) was slowly added a solution of Cu $(ClO_4)_2{\cdot}6H_2O$ (0.370 g, 1.0 mM) in 30 mL ethanol with stirring. The pH of the solution was adjusted to about 8 with triethylamine. After reluxing for 8 h, the mixture was cooled to room temperature and filtered. The filtrate was kept at room temperature. Three days later, blue cubic crystals suitable for X-ray analysis were obtained with 62% yield. Anal. Calcd for $C_{20}H_{30}Cl_2N_8O_{12}Cu_2$: C, 31.10; N, 14.51; H, 3.91%. Found: C, 30.92; N, 14.16; H, 4.23%. IR (KBr disk, cm^{-1}): 3439 (s, br), 3138 (m), 2375 (s), 2343 (s), 2301 (s), 1634 (s), 1597 (s), 1508 (m), 1342 (m), 1122 (s), 1073 (s), 752 (m), 667 (s), 626 (s), 416 (s).

2.4. *Synthesis of $[Cu(HL)_2(phen)](ClO_4)_2$ (2)*

To 10 mL methanol solution of HL (0.224 g, 2.0 mM) was slowly added a solution of Cu $(ClO_4)_2{\cdot}6H_2O$ (0.370 g, 1.0 mM) in 30 mL ethanol with stirring. After stirring for 30 min, 1,10-phenanthroline (0.180 g, 1.0 mM) was added. Then, after reluxing for 8 h, the mixture was cooled to room temperature and filtered. The filtrate was kept at room temperature. Three days later, blue cubic crystals suitable for X-ray analysis were obtained with 68% yield. Anal. Calcd for $C_{22}H_{24}Cl_2N_6O_{10}Cu$: C, 39.62; N, 12.60; H, 3.63%. Found: C, 39.46; N, 12.51; H, 3.91%. IR (KBr disk, cm^{-1}): 3407 (s, br), 3131 (m), 2367 (s), 1621 (s), 1524 (s), 1424 (s), 1342 (s), 1277 (m), 1222 (m), 1107 (s), 1068 (s), 926 (m), 847 (s), 766 (s), 720 (s), 672 (s), 620 (s).

2.5. *X-ray crystallography*

Single crystals of **1** and **2** were used for X-ray diffraction analyses by mounting on the tip of a glass fiber in air using a Bruker Smart Apex CCD diffractometer at 291 K with graphite-monochromated Mo Kα radiation ($\lambda = 0.71073$ Å). Diffraction intensities for the complexes were collected using the ω-scan technique. The structures were solved by direct methods using SHELXS-97 [20] and subsequent Fourier difference techniques, and refined anisotropically by full-matrix least-squares on F^2 using SHELXL-97 [21]. All nonhydrogen atoms were refined anisotropically and all hydrogens were located in the Fourier difference maps. Further crystallographic data and experimental details for structural analyses of **1** and **2** are summarized in table 1. Selected bond distances and angles are listed in table 2.

2.6. *DFT calculation*

The atomic coordinate positions of **1** and **2** were based on the data of the crystal structures, in which the solvent molecules and ClO_4^- were ignored. DFT calculations with a hybrid Functional B3LYP method at the LanL2DZ basis set were performed with Gaussian 98 software package [22]. In **1**, the charge and multiplicity is respectively set as +2, 3 with restricted-open spin due to two unpaired electrons in two copper(II), while +2, 2 in **2** because of one unpaired electron in Cu(II). All calculations were performed on a Pentium IV computer using the high convergence criteria. For **1**, 64 atoms, 392 basis functions, 1024 primitive gaussians, 138 alpha electrons, and 136 beta electrons are involved in the

Table 1. Crystal data, data collection, and structure refinement parameters for HL, **1**, and **2**.

Compound	HL	**1**	**2**
Empirical formula	$C_5H_8N_2O$	$C_{20}H_{30}Cl_2Cu_2N_8O_{12}$	$C_{22}H_{24}Cl_2CuN_6O_{11}$
Formula weight	112.13	772.50	682.91
Temperature (K)	293	293	293
λ/(Å)	0.71073	0.71073	0.71073
Crystal system	Orthorhombic	Monoclinic	Triclinic
Space group	*Pbca*	$P2_1/n$	$P-1$
a (Å)	12.3358(12)	7.3523(4)	8.0008(12)
b (Å)	7.0839(7)	10.7269(6)	12.0485(18)
c (Å)	13.1696(13)	18.9324(11)	15.977(2)
α (°)	90.00	90.00	83.140(2)
β (°)	90.00	91.2180(10)	76.398(2)
γ (°)	90.00	90.00	74.060(2)
Volume (Å^3), Z	1150.8(2), 8	1492.81(15), 1	1436.9(4), 2
Calculated density (Mg m^{-3})	1.294	1.719	1.578
Absorption coefficient (mm^{-1})	0.093	1.676	1.013
F(0 0 0)	480	788	698
θ Range for data collection (°)	3.09–27.44	2.15–27.67	1.76–25.35
Limiting indices	$-12 \le h \le 15$	$-9 \le h \le 9$	$-9 \le h \le 9$
	$-9 \le k \le 9$	$-13 \le k \le 13$	$-12 \le k \le 14$
	$-17 \le l \le 16$	$-24 \le l \le 23$	$-19 \le l \le 19$
Data/restraints/parameters	1310/0/76	3463/0/205	5211/0/392
Total reflections	9019	12,761	10,405
Unique reflections (R_{int})	0.0268	0.0259	0.0203
Completeness	99.8%	99.3%	98.7%
Goodness-of-fit on F^2	1.019	1.044	1.055
R_1/wR_2 [$I > 2\sigma(I)$]	0.0395/0.1102	0.0306/0.0815	0.0565/0.1652
R_1/wR_2 [all data]	0.0431/0.1144	0.0389/0.0865	0.0651/0.1727
$\Delta\rho_{max,\ min}$ (e Å^{-3})	0.239/−0.143	0.420/−0.364	0.625/−0.586

Table 2. Selected bond lengths (Å) and angles (°) for **1** and **2**.

1			
Cu(1)–O(1)	1.9350(15)	Cu(1)–N(2)	1.9523(17)
Cu(1)–O(1A)	1.9378(15)	Cu(1)–N(3)	1.9632(19)
O(1)–Cu(1)–O(1A)	78.11(7)	O(1)–Cu(1)–N3	82.61(7)
O(1)–Cu(1)–N2	176.76(7)	O(1A)–Cu(1)–N3	150.69(8)
O(1A)–Cu(1)–N2	99.73(7)	N2–Cu(1)–N3	100.29(8)
2			
Cu(1)–N(1)	1.977(4)	Cu(1)–N(6)	2.028(4)
Cu(1)–N(3)	1.981(4)	Cu(1)–N(5)	2.031(4)
N(1)–Cu(1)–N(3)	90.95(15)	N(1)–Cu(1)–N(5)	94.55(15)
N(1)–Cu(1)–N(6)	172.07(14)	N(3)–Cu(1)–N(5)	169.92(15)
N(3)–Cu(1)–N(6)	93.86(15)	N(6)–Cu(1)–N(5)	81.67(15)

Note: Symmetry transformations used to generate equivalent atoms for **1**: A, $-x+1, -y+2, -z$.

calculation. For **2**, 55 atoms, 340 basis functions, 898 primitive gaussians, 116 alpha electrons, and 116 beta electrons are involved in the calculation.

2.7. *Cyclic voltammetry*

A CHI400c computerace instrument was employed to obtain cyclic voltammograms in dimethylformamide solutions of the complex (1 mM) at room temperature (298 K) under nitrogen using 0.1 M tetrabutylammonium perchlorate (TBAP) as supporting electrolyte. A glass carbon working electrode, a platinum auxiliary electrode, and a Ag/AgCl reference electrode were used to obtain cyclic voltammograms. Measured potentials were calibrated through an internal ferrocene (Fc^+/Fc) standard.

2.8. *SOD-like activity*

Superoxide anion ($O_2^{\cdot-}$) was generated in an enzymatic (xanthine/xanthine oxidase) system in the presence or absence of test complex, and $O_2^{\cdot-}$ production was determined by monitoring the reduction of NBT to monoformazan dye at 560 nm at 298 ± 0.1 K [23–26]. An appropriate amount of xanthine oxidase was added to a mixture of 500 μM NBT, 500 μM xanthine, and 0–1.0 μM complex dissolved in 50 mM phosphate buffer (pH 7.8) to cause a variation of absorbance ($\Delta A_{560}/\Delta t_{min}$) of 0.025 ± 0.005. The percentage inhibition (% *I*) of NBT^+ formation was calculated from equation: (%) $I = (A_0 - A_s)/A_0 \times 100$, in which A_0 and A_s are the maximum absorbance values due to NBT^+ at 560 nm in the absence and in the presence of the complex. By plotting the % *I* as a function of complex concentration, the IC_{50} values were calculated.

3. Results and discussion

3.1. *UV–vis, IR spectroscopy of 1 and 2*

The electronic absorption spectra of **1** and **2** in freshly prepared methanol solution were obtained from 200 to 1100 nm at room temperature. As shown in figure S1 (see online supplemental material at http://dx.doi.org/10.1080/00958972.2014.940335), the electronic spectra of free HL displayed intense absorption at 221 nm due to an $n \rightarrow \pi^*$ transition, which was shifted to 216 and 232 nm for **1** and **2**, respectively. The broad band at 303 nm in **1**

was assigned to the ligand-to-metal charge transfer (LMCT) transition. The band at 295 nm in **2** was assigned to LMCT transition. The low energy bands at 500–1000 nm corresponded to *d–d* transitions. The broad band at 811 nm increased and shifted to 725 and 642 nm for **1** and **2**, respectively, indicating that copper(II) binds with the ligand. As shown in figure S2, IR spectra show absorptions at 3440 cm^{-1} for **1** and 3410 cm^{-1} for **2**, which can be attributed to the stretching vibrations of O–H. Absorptions at 3148 cm^{-1} for **1** and 3125 cm^{-1} for **2** originate from stretching vibrations of imidazole–H. The peak at 1634 cm^{-1} was assigned to the C=C stretching frequency. The bands around 1508 and 1342 cm^{-1} were attributed to ν(C=N) and ν(C–N), respectively. Most important, the strong bands at 1122 and 626 cm^{-1} for **1** (**2** at 1096 and 615 cm^{-1}) can be ascribed to vibration of perchlorate in the copper(II) complexes [27–29].

3.2. *Crystal structure analysis*

Ligands **1** and **2** have been structurally characterized by X-ray crystallography (figure 1). The single-crystal X-ray analysis reveals that $[Cu_2(HL)_2(L)_2](ClO_4)_2$ (**1**) crystallizes in the monoclinic space group $P2_1/n$ and exhibits a dinuclear structure, which contains two Cu(II) centers, two L^- anions, two [HL], and two non-coordinated perchlorates. Selected bond lengths and angles are listed in table 2. Each copper ion is at the center of the N_2O_2 donor set derived from three ligands in a square-planar geometry with Cu1 deviation 0.2320(2) Å out from the plane. The two bridged oxygens and two copper(II) ions are practically coplanar with deviations from the least-squares plane lower than 0.002(1) Å. The dihedral angle between the N_2O_2 plane and Cu_2O_2 plane is 23.2(1)°. The bond length of Cu1–O1(1.938 (2) Å) is typical for Cu–O complexes, while those of Cu–N (Cu(1)–N(2), 1.952(2) Å; Cu (1)–N(3), 1.963(2) Å) are also in the normal range [30–32]. The distance of the Cu(1)···O (2) (2.430(2) Å) is obviously longer than that of Cu(1)–O(1), due to O(2) from the alcohol hydroxyl whereas O1 is from the deprotonated alcohol hydroxyl. Therefore, Cu(1) is four-coordinate by O(1), O(1A), N(2), and N(3). The conformation of the dinuclear copper(II) ions and four ligands is centrosymmetric, resulting in uniform coordination for each copper (II). The Cu···Cu distance in each binuclear complex is 3.007 Å, close to that commonly observed in dinuclear copper(II) complex based on the Robson-type macrocycle ligand [33]. $[Cu(HL)_2(phen)](ClO_4)_2$ (**2**) crystallizes in the monoclinic space group $P-1$. Its asymmetric unit contains one Cu^{2+}, two HL, one 1,10-phenanthroline, and two uncoordinated perchlorates. As shown in figure 1(3), each Cu^{2+} is coordinated by two nitrogens from 1,10-phenanthroline and two nitrogens from two HL. The coordination environment of Cu(II) can be regarded as a slightly distorted planar geometry.

3.3. *DFT calculation*

By analysis of Mulliken population, some information of atom net charges of **1** and **2** were obtained (table 3). The net charge of Cu(II) is less than the original value (+2). In **1**, the net negative charge of O(1), O(1A), N(2), and N(3) are higher than that of O(2), N(1), and N (4), suggesting that copper ion was preferentially coordinated by two oxygens from deprotonated hydroxyl and two nitrogens from two imidazole groups. For **2**, the net negative charges of O(1), O(2), N(2), and N(4) are obviously lower than that of other N atoms, indicating that the above two hydroxyl oxygens from two ligands did not take part in complexation. The frontier molecular orbital energies of **1** and **2** are listed in table 4, where the

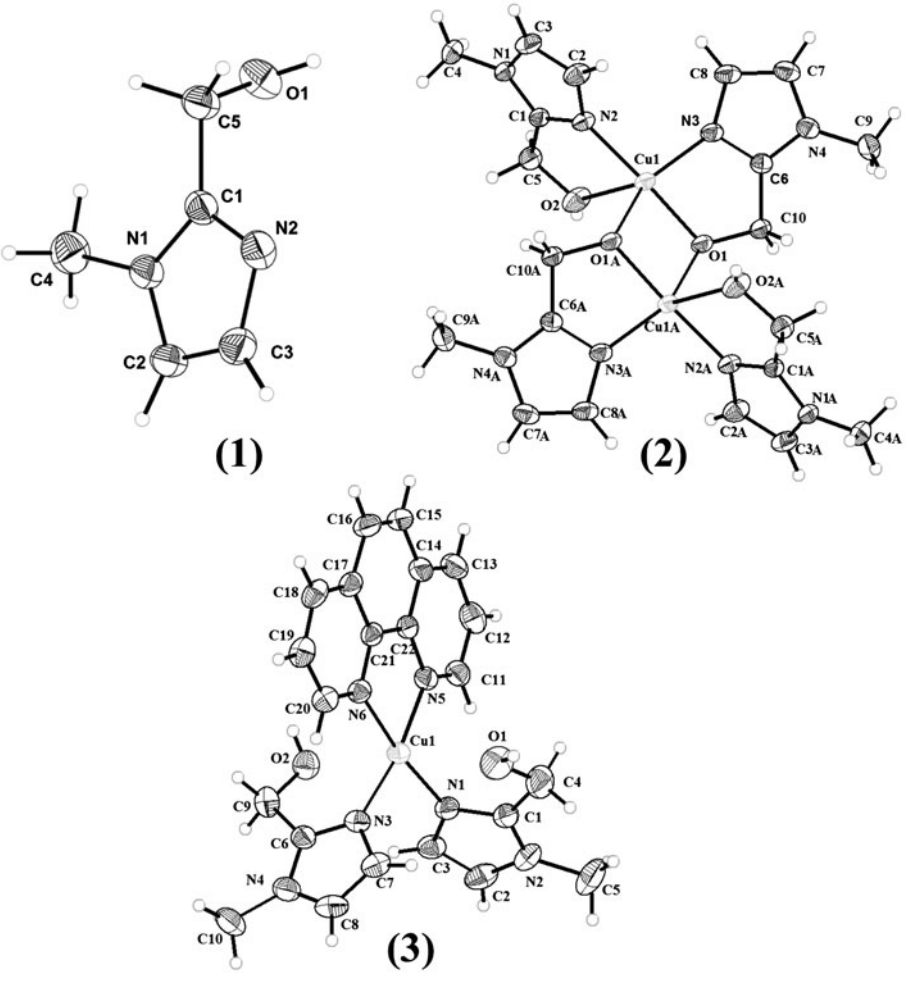

Figure 1. (1) ORTEP view of (*N*-methyl-2-methylol)imidazole (HL). Thermal ellipsoids are drawn at 30% probability level. (2) ORTEP view of $[Cu_2(HL)_2(L)_2](ClO_4)_2$. Thermal ellipsoids are drawn at 30% probability level. The "A" labeled atoms are at equivalent positions $(-x+1, -y+2, -z)$. (3) ORTEP view of $[Cu(HL)_2(phen)](ClO_4)_2$. Thermal ellipsoids are drawn at 30% probability level.

occupied molecular orbital energies are all negative, indicating the complex is stable. Compared with that of **2**, the energy difference ($\Delta E = E_{LUMO} - E_{HOMO}$) of **1** is lower, indicating that copper ion of **1** has a stronger potential of accepting lone electron pair of $O_2^{\cdot-}$ as an active center of the antioxidative reagent [34].

3.4. *Cyclic voltammetry*

The electrochemical properties of **1** and **2** have been studied by cyclic voltammetry (CV) in degassed DMF solution under nitrogen using 0.1 M TBAP as supporting electrolyte. A glass carbon working electrode, a platinum auxiliary electrode, and a Ag/AgCl reference

Table 3. Mulliken atomic charges of some atoms of **1** and **2** at the B3LYP/LanL2DZ level.

1		**2**	
Atom	Charge	Atom	Charge
Cu(1)	1.3057	Cu(1)	1.3475
N(1)	−0.3944	N(1)	−0.5652
N(2)	−0.6026	N(2)	−0.3544
N(3)	−0.5900	N(3)	−0.5792
N(4)	−0.3800	N(4)	−0.3331
O(1)	−0.9391	N(5)	−0.5250
O(2)	−0.2154	N(6)	−0.5053
		O(1)	−0.2485
		O(2)	−0.2460

Table 4. Frontier molecular orbital energies (eV) of **1** and **2** at the B3LYP/LanL2DZ level.

Energies (eV)	**1**	**2**
HOMO	−6.3342	−7.1915
LUMO	−4.7723	−4.3922
ΔE	1.5619	2.7993

electrode were used to obtain cyclic voltammograms. Under these conditions, the Fc^+/Fc standard couple occurred at 544 mV, identical to that reported previously [35]. The data for **1** and **2** are collected in table 5 and the cyclic voltammograms of the complexes are shown in figure 2. Complex **1** showed the *quasi*-reversible redox waves with $E_{1/2} = 0.28$ V *versus* Fc^+/Fc, $\Delta E_p = 0.12$ V, and $i_{pa}/i_{pc} = 1.06$, which was typical of reversible Cu(II)/Cu(I) process for the dinuclear copper(II) complex. The CV of **2** exhibits one reversible one-electron redox couple at $E_{1/2} = 0.13$ V *versus* Fc^+/Fc, $\Delta E_p = 0.09$ V. It should be pointed out that only one pair of redox peaks was detected in the dinuclear **1**, indicating that the environments of the two copper ions are very similar [34, 36]. It is in agreement with the centrosymmetric conformation of the dicopper complex from crystal structure analysis. The potentials of **1** can be assigned to one-electron process for each Cu(II)/Cu(I) couple and two-electron process for the dinuclear copper(II) complex. The difference in Cu(II)/Cu(I) redox potential between **1** and **2** demonstrates that the coordination environments around the copper(II) ions of the two complexes are different. An adequate Cu(II)/Cu(I) redox potential for effective catalysis of superoxide radical must be required between −0.36 V *versus* Ag/AgCl for O_2/O_2^- and 0.69 V *versus* Ag/AgCl for O_2^-/H_2O_2 [15]. Therefore, **1** and **2** can be applied to mimic superoxide dismutase, because the redox potentials of the two complexes in DMF were located in the allowed ranges of an SOD mimic.

Table 5. Redox potential data *vs.* Fc^+/Fc for 10^{-3} M solution of **1** and **2** in DMF containing 0.1 M TBPA and scan rate 100 mV s^{-1}.

Complex	E_{pa}/V	E_{pc}/V	$E_{1/2}/V$	$\Delta E/V$
1	0.34	0.22	0.28	0.12
2	0.17	0.08	0.13	0.09

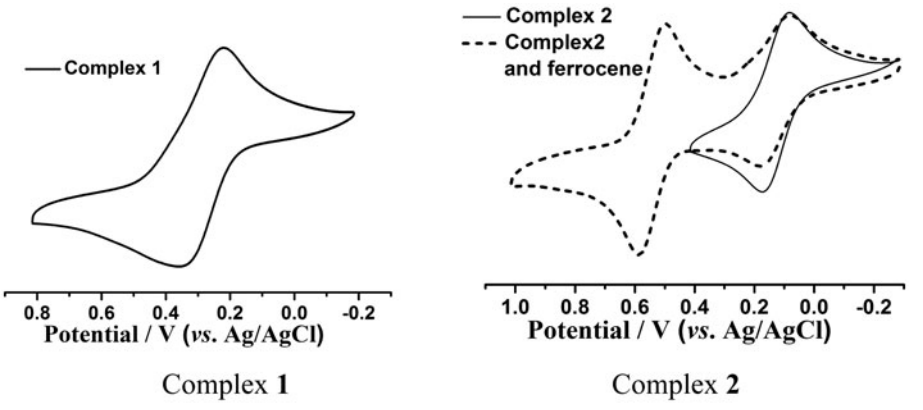

Figure 2. Cyclic voltammograms of **1** and **2** in DMF at 298 K and 100 mV s^{-1} scan rate.

3.5. *Electronspray ionization mass spectrometry*

To prove the state of **1** and **2** in the phosphate buffer solutions at pH 7.8, mass spectra (ESI, positive-detection mode) were performed. Sample solutions were injected into the ion source with the addition of methanol at a flow rate of 5 mL min^{-1}. As shown in figure S3, for **1**, the prominent peak at 286.67 *m/z* was assigned to the $[Cu_2(HL)_2(L)_2]^{2+}$ double-charge positive species, due to loss of the two non-coordinated perchlorate anions. The peaks at 113.33, 135.42, 323.25, 398.00, and 461.17 *m/z* may be related to $[HL + H]^+$, $[HL + Na]^+$, $[Cu_2(HL)_2(L)_2 + 4H_2O]^{2+}$, $[Cu_2(HL)_4(L)_2]^{2+}$, and $[Cu_2(HL)_2(L)_2 + 4\ MeOH]^{2+}$, respectively. As for **2**, the peaks at 113.25 and 181.50 *m/z* are attributed to HL and phen, respectively. The prominent peak for **2** at 354.50 *m/z* corresponds to $[Cu(L)(phen)]^+$, due to the hydroxyl deprotonation of HL at pH 7.8 and further providing the coordination of oxygen, resulting in the loss of one HL from $[Cu(HL)_2(phen)]^{2+}$. The peak at 423.25 *m/z* can be ascribed to the solvent adduct $[Cu(L)(phen)+2H_2O + 2MeOH]^+$.

3.6. *SOD-like activity*

The SOD-like (SOD = superoxide dismutase) activities of **1** and **2** were investigated by NBT assay [23–26]. The imidazole derivative with a hydroxymethyl arm provides a hydrophilic environment similar to that in the active site of the native enzyme. The concentrations of the complex required to attain 50% inhibition of the reduction (defined as IC_{50}) were determined, and IC_{50} value of bovine erythrocyte SOD is 0.042 ± 0.01 μM, almost identical to 0.04 μM value reported [37]. From the control experiments of copper(II) perchlorate, the IC_{50} values of free copper(II) is 4.01 μM, which is very close to that reported previously [38]. The ligand did not exhibit $O_2^{\cdot-}$ scavenger effects under the same conditions (IC_{50} > 1000 μM). As shown in figure 3, IC_{50} values of **1** and **2** at pH 7.8, obtained from the plot of inhibition percentage *versus* copper(II) ion concentration, are 0.10 and 0.19 μM, respectively. Despite the lower activity than the native enzyme, **1** and **2** are among the relatively active model compounds of SOD enzyme [39, 40]. The difference in IC_{50} values for the two complexes should be ascribed to different structures between **1** and **2**. For **2**, the CuN_4 coordination is different from that of the natural enzyme. Meanwhile, phenanthroline as the rigid co-ligand in **2** is unfavorable for accommodating the geometrical transformation from

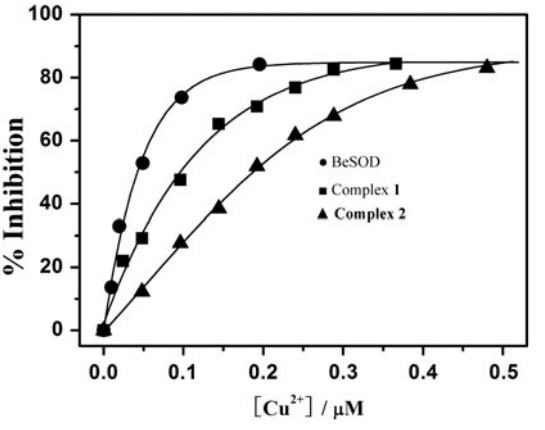

Figure 3. Percentage of inhibition of superoxide radicals by NBT^+ absorption at 560 nm in the presence of bovine erythrocyte SOD (BeSOD) (●), **1** (■), and **2** (▲) at pH 7.8 phosphate buffer.

Cu(II) to Cu(I) during the catalytic process. The higher activity of **1** may be attributed to the two labile hydroxymethyl groups in the coordination, which are proposed to be easily substituted by O_2^- in the catalytic process [15], which is similar to $O_2^{\cdot-}$ displacing water bound to the copper site in the mechanism of $O_2^{\cdot-}$ dismutation by native SOD [40–42].

4. Conclusion

We report the syntheses, structures, and properties of two new copper(II) complexes based on imidazole with a hydroxymethyl pendant, $[Cu_2(HL)_2(L)_2](ClO_4)_2$ (**1**) and $[Cu(HL)_2(phen)](ClO_4)_2$ (**2**). The *quasi*-reversible Cu(II)/Cu(I) redox waves of **1** and **2** were determined by cyclic voltammetry. The atomic net charges distribution and frontier molecular orbital energies were obtained by calculation. Complex **1** exhibits high SOD-like activity, which can be attributed to the CuN_2O_2 coordination configuration and the labile hydroxymethyl pendants.

Supplementary material

Crystallographic data for HL, **1** and **2** have been deposited with the Cambridge Crystallographic Data Center as supplementary publication CCDC reference numbers 959840, 959839 and 981394, respectively. These data can be obtained free of charge via http://www.ccdc.cam.ac.uk/conts/retrieving.html, or from the Cambridge Crystallographic Data Center, 12 Union Road, Cambridge CB2 1EZ, UK; Fax: (+44) 1223 336 033; or Email: deposit@ccdc.cam.ac.uk.

Funding

This work was supported by the National Natural Science Foundation of China [grant number 20901002].

References

[1] G. Bauer. *Anticancer Res.*, **32**, 2599 (2012).
[2] A.F. Chen, D.D. Chen, A. Daiber, F.M. Faraci, H.G. Li, C.M. Rembold, I. Laher. *Clin. Sci.*, **123**, 73 (2012).
[3] J.E. Slemmer, I.J. Shacka, M.I. Sweeney, J.T. Weber. *Curr. Med. Chem.*, **15**, 404 (2008).
[4] K. Jomova, M. Valko. *Toxicology*, **283**, 65 (2011).
[5] H. Zhang, C. Andrekopoulos, J. Joseph, J. Crow, B. Kalyanaraman. *Free Radical Biol. Med.*, **36**, 1355 (2004).
[6] D. Salvemini, Z.-Q. Wang, J. Zweier, A. Samouilov, H. Macarthur, T. Misko, M.G. Currie, S. Cuzzocrea, J.A. Sikorski, D.P. Riley. *Science*, **286**, 304 (1999).
[7] V. Balasubramanian, M. Ezhevskaya, H. Moons, M. Neuburger, C. Cristescu, S. Van Doorslaer, C. Palivan. *Phys. Chem. Chem. Phys.*, **11**, 6778 (2009).
[8] G. Ferrer-Sueta, L. Ruiz-Ramírez, R. Radi. *Chem. Res. Toxicol.*, **10**, 1338 (1997).
[9] K. Jitsukawa, M. Harata, H. Arii, H. Sakurai, H. Masuda. *Inorg. Chim. Acta*, **324**, 108 (2001).
[10] T. Fukuuchi, K. Doh-Ura, S. Yoshihara, S. Ohta. *Bioorg. Med. Chem. Lett.*, **16**, 5982 (2006).
[11] R. Belda, S. Blasco, B. Verdejo, H.R. Jiménez, A. Doménech-Carbó, C. Soriano, J. Latorre, C. Terencio, E. García-España. *Dalton Trans.*, **42**, 11194 (2013).
[12] L.S. Long, K.Y. Ding, X.M. Chen, L.N. Ji. *Inorg. Chem. Commun.*, **3**, 65 (2000).
[13] Q. Raffy, R. Ricoux, E. Sansiaume, S. Pethe, J.P. Mahy. *J. Mol. Catal. A: Chem.*, **317**, 19 (2010).
[14] T.M. Rajendiran, M.T. Caudle, M.L. Kirk, I. Setyawati, J.W. Kampf, V.L. Pecoraro. *J. Biol. Inorg. Chem.*, **8**, 283 (2003).
[15] D. Li, S. Li, D. Yang, J. Yu, J. Huang, Y. Li, W. Tang. *Inorg. Chem.*, **42**, 6071 (2003).
[16] T. Koike, S. Kajitani, I. Nakamura, E. Kimura, M. Shiro. *J. Am. Chem. Soc.*, **117**, 1210 (1995).
[17] T.G. Sprigings, C.D. Hall. *J. Chem. Soc., Perkin Trans.*, **2**, 2063, (2001).
[18] C. Liao, N. Shao, K.S. Han, X.-G. Sun, D.-E. Jiang, E.W. Hagaman, S. Dai. *Phys. Chem. Chem. Phys.*, **13**, 21503 (2011).
[19] D.Q. Nguyen, H.W. Bae, E.H. Jeon, J.S. Lee, M. Cheong, H. Kim, H.S. Kim, H. Lee. *J. Power Sources*, **183**, 303 (2008).
[20] G.M. Sheldrick. *SHELXS 97*, University of Gottingen, Gottingen, Germany (1997).
[21] G.M. Sheldrick. *SHELXL 97*, University of Gottingen, Gottingen, Germany (1997).
[22] M.J. Frisch, G.W. Trucks, H.B. Schlegel, G.E. Scuseria, M.A. Robb, J.R. Cheeseman, V.G. Zakrzewski, J.A. Montgomery Jr., R.E. Stratmann, J.C. Burant, S. Dapprich, J.M. Millam, A.D. Daniels, K.N. Kudin, M.C. Strain, O. Farkas, J. Tomasi, V. Barone, M. Cossi, R. Cammi, B. Mennucci, C. Pomelli, C. Adamo, S. Clifford, J. Ochterski, G.A. Petersson, P.Y. Ayala, Q. Cui, K. Morokuma, P. Salvador, J.J. Dannenberg, D.K. Malick, A.D. Rabuck, K. Raghavachari, J.B. Foresman, J. Cioslowski, J.V. Ortiz, A.G. Baboul, B.B. Stefanov, G. Liu, A. Liashenko, P. Piskorz, I. Komaromi, R. Gomperts, R.L. Martin, D.J. Fox, T. Keith, M.A. Al-Laham, C.Y. Peng, A. Nanayakkara, M. Challacombe, P.M.W. Gill, B. Johnson, W. Chen, M.W. Wong, J.L. Andres, C. Gonzalez, M. Head-Gordon, E.S. Replogle, J.A. Pople. *Gaussian Inc.*, Pittsburgh, PA, Gaussian (1998).
[23] Y.H. Zhou, H. Fu, W.X. Zhao, W.L. Chen, C.Y. Su, H. Sun, L.N. Ji, Z.W. Mao. *Inorg. Chem.*, **46**, 734 (2007).
[24] Y.H. Zhou, J. Chen, Y.J. Shang, Y. Cheng. *J. Inclusion Phenom. Macrocyclic Chem.*, **74**, 343 (2012).
[25] M. Safavi, A. Foroumadi, M. Nakhjiri, M. Abdollahi, A. Shafiee, H. Ilkhani, M.R. Ganjali, S.J. Hosseinimehr, S. Emami. *Bioorg. Med. Chem. Lett.*, **20**, 3070 (2010).
[26] A. Barik, B. Mishra, L. Shen, H. Mohan, R.M. Kadam, S. Dutta, H.Y. Zhang, K.I. Priyadarsini. *Free Radical Biol. Med.*, **39**, 811 (2005).
[27] A. Ramadan. *J. Coord. Chem.*, **65**, 1417 (2012).
[28] J.P. Naskar, B. Guhathakurta, L.P. Lu, M.L. Zhu. *Polyhedron*, **43**, 89 (2012).
[29] C.H. He, C.H. Jiao, J.C. Geng, G.H. Cui. *J. Coord. Chem.*, **65**, 2294 (2012).
[30] O. Piovesana, B. Chiari, A. Cinti, A. Sulpice. *Eur. J. Inorg. Chem.*, **2011**, 4414 (2011).
[31] J. Haníková, J. Černák, J. Kuchár, E. Čižmár. *Inorg. Chim. Acta*, **385**, 178 (2012).
[32] J.H. Choi, M.D.A. Subhan, S.W. Ng. *J. Coord. Chem.*, **65**, 3481 (2012).
[33] W.D. Carlisle, D. Fenton, P. Roberts, U. Casellato, P. Vigato, R. Graziani. *Transition Met. Chem.*, **11**, 292 (1986).
[34] Y.-H. Zhou, W.-Q. Wan, D.-L. Sun, J. Tao, L. Zhang, X.-W. Wei. *Z. Anorg. Allg. Chem.*, **640**, 249 (2014).

[35] I. Noviandri, K.N. Brown, D.S. Fleming, P.T. Gulyas, P.A. Lay, A.F. Masters, L. Phillips. *J. Phys. Chem. B*, **103**, 6713 (1999).
[36] V. Sargentelli, A.V. Benedetti, A.E. Mauro. *J. Braz. Chem. Soc.*, **8**, 271 (1997).
[37] U. Weser, L.M. Schubotz, E. Lengfelder. *J. Mol. Catal.*, **13**, 249 (1981).
[38] M. Safavi, A. Foroumadi, M. Nakhjiri, M. Abdollahi, A. Shafiee, H. Ilkhani, M.R. Ganjali, S.J. Hosseinimehr, S. Emami. *Bioorg. Med. Chem. Lett.*, **20**, 3070 (2010).
[39] R. Buchtík, Z. Trávníček, J. Vančo. *J. Inorg. Biochem.*, **116**, 163 (2012).
[40] H. Fu, Y.H. Zhou, W.L. Chen, Z.G. Deqing, M.L. Tong, L.N. Ji, Z.W. Mao. *J. Am. Chem. Soc.*, **128**, 4924 (2006).
[41] R.J. Sanchez, C. Srinivasan, W.H. Munroe, M.A. Wallace, J. Martins, T.Y. Kao, K. Le, E.B. Gralla, J.S. Valentine. *J. Biol. Inorg. Chem.*, **10**, 913 (2005).
[42] M.C. Carroll, J.B. Girouard, J.L. Ulloa, J.R. Subramaniam, P.C. Wong, J.S. Valentine, V.C. Culotta. *Proc. Natl. Acad. Sci.*, **101**, 5964 (2004).